CARDIAC MOTION ESTIMATION IN ULTRASOUND IMAGES USING SPATIAL AND SPARSE REGULARIZATIONS

*N. Ouzir, J.-Y. Tourneret**

University of Toulouse
INP-ENSEEIHT/IRIT/TeSA,
2 rue Camichel
31071 Toulouse Cedex 7, France

*A. Basarab**

University of Toulouse
IRIT, CNRS UMR 5505
118 Route de Narbonne
31062 Toulouse Cedex 9, France

ABSTRACT

This paper investigates a new method for cardiac motion estimation in 2D ultrasound images. The motion estimation problem is formulated as an energy minimization with spatial and sparse regularizations. In addition to a classical spatial smoothness constraint, the proposed method exploits the sparse properties of the cardiac motion to regularize the solution via an appropriate dictionary learning step. The proposed method is evaluated in terms of motion estimation and strain accuracy and compared with state-of-the-art algorithms using a dataset of realistic simulations. These simulation results show that the proposed method provides very promising results for myocardial motion estimation.

Index Terms— Ultrasound imaging, dictionary learning, motion estimation, sparse representations, cardiac imaging.

1. INTRODUCTION

Cardiovascular diseases are one of the main causes of death around the world. In this context, it is important to improve the techniques used for the diagnosis of cardiac malfunction. Ultrasound imaging (UI) is one of the most widely used medical imaging modalities in cardiology. This modality has many advantages such as patient confort, low budget requirements and high temporal resolution. More specifically, automatic cardiac motion and strain estimation from ultrasound (US) images have been proved to be efficient tools for the diagnosis of cardiovascular diseases [1].

Cardiac motion estimation techniques can be classified into three main categories. First, optical flow (OF) algorithms are based on differential methods and use the pixel intensity constancy assumption [2]. The second category includes the so-called speckle tracking methods, which consist in matching blocks of two consecutive images using a similarity measure. Finally, in elastic registration, motion is introduced as a global parametric or discrete deformation map [3]. In order to overcome the ill-posed nature of motion estimation (characterized by the absence of a unique solution), many estimation methods introduce additional constraints to regularize the estimation problem. These constraints can be based on spatial or temporal smoothness [4] or use specific parametric motion models. In particular, B-spline regularization has shown interesting results for cardiac motion estimation [5].

In recent works, sparse representations have been successfully considered to regularize a wide variety of problems [6, 7]. In particular, sparsity can be introduced by expressing an unknown signal $\boldsymbol{u} \in \mathbb{R}^N$ as a weighted linear combination of a few elements of an overcomplete dictionary $\boldsymbol{D} \in \mathbb{R}^{n\times q}$. In the context of 2D signals, *e.g.*, for motion fields or images, the so-called sparse coding problem is generally formulated patch-wise as

$$\min_{\boldsymbol{\alpha}_p} \|\boldsymbol{\alpha}_p\|_0 \text{ subject to } \|\boldsymbol{P}_p\boldsymbol{u} - \boldsymbol{D}\boldsymbol{\alpha}_p\|_2^2 < \epsilon \qquad (1)$$

where $\|.\|_0$ is the l_0 *pseudo-norm*, which counts the number of non-zero elements of a vector, $\boldsymbol{P}_p \in \mathbb{R}^{n\times N}$ is a binary operator that extracts the pth patch from $\boldsymbol{u}$, $\boldsymbol{\alpha}_p \in \mathbb{R}^q$ is the corresponding sparse vector and ϵ is a constant that needs to be fixed *a priori*. Although the problem (1) is NP-hard, it can be solved using algorithms that provide good solutions in polynomial time, such as the orthogonal matching pursuit (OMP) [8] or the least absolute shrinkage and selection operator (LASSO), which relaxes the l_0-minimization problem to an l_1-minimization [9].

The choice of an appropriate dictionary $\boldsymbol{D}$ is important. The dictionary can be predefined, *e.g.*, based on wavelets, discrete cosine transforms (DCT) or Fourier decompositions. However, data-driven dictionaries have been shown to outperform the predefined ones in specific applications [10]. Dictionary learning (DL) methods are based on a joint optimization problem with respect to the dictionary $\boldsymbol{D}$ and the sparse coefficient vectors $\boldsymbol{\alpha_p}$. In the context of a global motion field $\boldsymbol{u} \in \mathbb{R}^N$, the DL problem can be formulated as follows

$$\min_{\boldsymbol{D},\boldsymbol{\alpha_p}} \sum_p \|\boldsymbol{P}_p\boldsymbol{u} - \boldsymbol{D}\boldsymbol{\alpha}_p\|_2^2 \text{ subject to } \forall p, \|\boldsymbol{\alpha}_p\|_0 \leq K \quad (2)$$

*Part of this work has been supported by the thematic trimester on image processing of the CIMI Labex, Toulouse,France, under grant ANR-11-LABX-0040-CIMI within the program ANR-11-IDEX-0002-02.

where K is the maximum number of non-zero coefficients of $\boldsymbol{\alpha}_p$. Typical algorithms designed for solving (2) include the K-SVD [11] and online DL (ODL) algorithms [10].

At this point, it is interesting to mention that a few recent attempts to use sparse representations and DL for motion estimation have been investigated in the literature. In [12], the authors included a sparsity prior to an OF estimation problem and used the wavelet basis for the sparse coding step. This approach was also investigated in [13] using a learned motion dictionary. The method proposed in this paper combines a specific similarity measure for UI with spatial smoothness and sparse regularizations. This strategy exploits jointly the statistical properties of the speckle noise and the smooth and sparse properties of the cardiac motion. More precisely, we consider a multiplicative Rayleigh noise model introduced in [14][1], a spatial regularization based on the l_2-norm of the motion gradient and introduce a regularization exploiting a DL-based sparse representation of the cardiac motion.

The paper is organized as follows. Section 2 formulates the cardiac motion estimation problem and introduces the proposed strategy based on a sparse regularization. Some implementation details are provided in Section 3. Simulation results are presented and discussed in Section 4. In particular, the proposed method is evaluated on two sequences of highly realistic simulations and compared with two state-of-the-art algorithms: (i) a classical and widely used speckle tracking method, *i.e.*, the conventional block-matching (BM) [15], using the normalized cross-correlation (NCC) and (ii) an elastic registration method using a B-spline parameterization [3]. Concluding remarks are finally reported in Section 5.

2. MOTION ESTIMATION

We consider the estimation of a 2D displacement field between a pair of consecutive images $(\boldsymbol{r}_k, \boldsymbol{r}_{k+1}) \in \mathbb{R}^N \times \mathbb{R}^N$ acquired at time instants k and $k+1$. The motion field between these two images is denoted as $(\boldsymbol{u}, \boldsymbol{v})^T \in \mathbb{R}^N \times \mathbb{R}^N$, where the subscript k has been omitted for simplicity. In the proposed motion estimation method we seek to exploit the sparse properties of the motion field when it is decomposed on a suitable dictionary. We propose to make use of this idea by estimating the motion vector $\boldsymbol{u}$ (resp. $\boldsymbol{v}$) and the sparse coefficient vector $\boldsymbol{\alpha}_p$ through the minimization of the following cost function, composed of an energy $E_{\text{data}}(\boldsymbol{u})$ penalized by sparse and spatial regularization terms

$$\min_{\boldsymbol{\alpha}_p, \boldsymbol{u}} \{E_{\text{data}}(\boldsymbol{u}) + \lambda_d E_{\text{sparse}}(\boldsymbol{u}, \boldsymbol{\alpha_p}) + \lambda_s E_{\text{spatial}}(\boldsymbol{u})\} \quad (3)$$

where $\lambda_d \in \mathbb{R}^+$ and $\lambda_s \in \mathbb{R}^+$ are two regularization parameters allowing the importance of the two regularization terms to be controlled [16]. In this work, the problem is written independently for the horizontal and vertical components $\boldsymbol{u}$ and $\boldsymbol{v}$. Note that the first term in (3) is also referred to as the data fidelity term, which expresses the similarity between the displaced image $\boldsymbol{r}_{k+1}$ and the reference image $\boldsymbol{r}_k$. On the other hand, the two regularization terms E_{sparse} and E_{spatial} express the sparsity and the spatial coherence of the motion field. More details about these terms are provided in the following sections.

2.1. Data fidelity term

According to the maximum likelihood (ML) approach, the estimation of the motion $\boldsymbol{u}$ is achieved by maximizing the conditional probability density function of the observation $\boldsymbol{r}_{k+1}$ given $\boldsymbol{r}_k$ and $\boldsymbol{u}$, denoted as $p(\boldsymbol{r}_{k+1}|\boldsymbol{r}_k, \boldsymbol{u})$. The problem is usually reformulated in the negative log-domain leading to

$$\min_{\boldsymbol{u}} \; -\ln[p(\boldsymbol{r}_{k+1}|\boldsymbol{r}_k, \boldsymbol{u})]. \quad (4)$$

In the case of US images, classical intensity-based similarity measures, such as the sum of squared differences (SSD) or NCC suffer from the presence of speckle noise [17]. The Rayleigh multiplicative noise is a more appropriate and widely accepted noise model in UI [18]. As explained in [14, 16], this assumption leads to the following energy (resulting from (4))

$$E_{\text{data}}(\boldsymbol{u}) = -2d(\boldsymbol{u}) + 2\log[e^{2d(\boldsymbol{u})} + 1] + \text{cst} \quad (5)$$

where $d(\boldsymbol{u}) = \frac{1}{b}\sum_{n=1}^{N}[\boldsymbol{r}_{k+1}(n + \boldsymbol{u}(n)) - \boldsymbol{r}_k(n)]$, n indicates the pixel index, $\boldsymbol{u} = [u(1), ..., u(N)]^T$ is the full motion vector, $\boldsymbol{r}_k = [r_k(1), ..., r_k(N)]^T$ and $\text{cst} = -\log\left(2\sigma^4/b\right)$ is a constant depending on the scale parameter of the Rayleigh distribution $\sigma \in \mathbb{R}^+$ and on the linear gain b related to the formation of the log-compressed B-mode images and set to 1 as in [3].

2.2. Spatial regularization

The spatial regularization term ensures the smoothness of the motion estimate. A classical choice is $E_{\text{spatial}}(\boldsymbol{u}) = \phi(\nabla \boldsymbol{u})$, where ϕ is a penalty function and ∇ is the gradient operator. In this work, we use $\phi(.) = \| \,.\|_2^2$, which enforces weak spatial gradients on the two motion components and leads to the first-order spatial regularization term [19]

$$E_{\text{spatial}}(\boldsymbol{u}) = \|\nabla \boldsymbol{u}\|_2^2. \quad (6)$$

2.3. Sparse regularization

The proposed sparse regularization consists in finding the motion $\boldsymbol{u}$ that is best described by a few atoms of a dictionary that contains patterns of training motions. The sparse regularization is performed patch-wise, so that each patch of motion $\boldsymbol{P}_p\boldsymbol{u}$ is constrained to have a sparse representation with respect to the motion dictionary $\boldsymbol{D}$, *i.e.*,

$$E_{\text{sparse}}(\boldsymbol{u}) = \sum\nolimits_p \|\boldsymbol{P}_p\boldsymbol{u} - \boldsymbol{D}\boldsymbol{\alpha}_p\|_2^2 \quad (7)$$

[1] Other similarity measures based on optical flow or on different noise models could be considered as well.

where $\boldsymbol{\alpha}_p$ is the sparse coefficient vector associated with the pth patch [13].

The combination of (5), (6) and (7) results in an original motion estimation problem exploiting a Rayleigh noise model with spatial smoothness and sparsity constraints. The next section studies the optimization algorithm that has been investigated to solve (3).

3. OPTIMIZATION STRATEGY

3.1. Dictionary learning

We start by learning an offline dictionary $\boldsymbol{D}$ from patches of a set of training motion fields. In this work, the DL problem (2) has been solved using the ODL algorithm, which iterates between a sparse coding step ($\boldsymbol{D}$ fixed) and a dictionary update step ($\boldsymbol{\alpha}_p$ fixed). Once the dictionary $\boldsymbol{D}$ has been learned, it is fixed and used for the motion estimation step described in the next section[2].

3.2. Cardiac motion estimation

Using the data fidelity and regularization terms detailed in Section 2, the cardiac motion estimation reduces to the following optimization problem

$$\min_{\boldsymbol{\alpha}_p,\boldsymbol{u}} \left\{ E_{\text{data}}(\boldsymbol{u}) + \lambda_d \sum\nolimits_p \|\boldsymbol{P}_p\boldsymbol{u} - \boldsymbol{D}\boldsymbol{\alpha}_p\|_2^2 + \lambda_s \|\nabla \boldsymbol{u}\|_2^2 \right\} \tag{8}$$
$$\text{subject to } \forall p,\ \|\boldsymbol{\alpha}_p\|_0 \leq K$$

where E_{data} has been defined in (5) and $\boldsymbol{D}$ has been determined offline as described in Section 3.1. Since (8) is hard to solve directly, we adopt an alternate minimization scheme, similar to the half quadratic splitting strategy employed in [20]. For fixed values of λ_d and λ_s, we alternate optimizations with respect to $\boldsymbol{\alpha}_p$ and $\boldsymbol{u}$. This process is repeated during a few iterations (typically 4 or 5 [20]) after which the sparsity parameter λ_d is increased. More details about these two steps are provided below.

3.2.1. Sparse coding

Two classes of algorithms have been investigated in the literature to solve sparse coding problems similar to (1). These algorithms are based on greedy strategies or on convex relaxation methods, which relax the l_0-minimization problem to an l_1-minimization. This paper focuses on the OMP algorithm solving the following problem [8]

$$\min_{\boldsymbol{\alpha_p}} \sum\nolimits_p \|\boldsymbol{P}_p\boldsymbol{u} - \boldsymbol{D}\boldsymbol{\alpha}_p\|_2^2 \text{ subject to } \forall p,\ \|\boldsymbol{\alpha}_p\|_0 \leq K \tag{9}$$

where p indicates the patch index and K is the maximum number of non-zero coefficients.[3]

[2]Note that the dictionary $\boldsymbol{D}$ could be updated jointly with the sparse coefficients in an adaptive way [16]. However, we have not observed significant improvements with this adaptive scheme for cardiac motion estimation in UI.

[3]Note that the LASSO algorithm was also considered for sparse coding. However, the obtained results did not change significantly compared to OMP.

3.2.2. Motion field estimation

Once the sparse codes and the dictionary have been determined, the motion field $\boldsymbol{u}$ is updated (starting from a first initialization $\boldsymbol{u}_0 = 0$) by solving the following problem

$$\min_{\boldsymbol{u}} \left\{ E_{\text{data}}(\boldsymbol{u}) + \lambda_d \sum\nolimits_p \|\boldsymbol{P}_p\boldsymbol{u} - \boldsymbol{D}\boldsymbol{\alpha}_p\|_2^2 + \lambda_s \|\nabla \boldsymbol{u}\|_2^2 \right\}. \tag{10}$$

The solution to (10) can be found by equating the gradient to zero, and following the optimization approach studied in [3].

4. EXPERIMENTAL RESULTS

This section evaluates the performance of the proposed method using a sparse representation and DL for cardiac motion estimation. The experiments were conducted on a dataset resulting from realistic simulations with known ground-truth. The performance of the proposed method is compared to two state-of-the-art motion estimation methods including the BM algorithm using the NCC similarity measure and an image registration method based on a B-spline motion parameterization [3]. Note that the B-spline algorithm uses the same similarity measure [14] and spatial regularization as the proposed method. In order to highlight the influence of the proposed combination of sparse and spatial regularizations, the proposed approach is also contrasted with the use of the spatial and sparse regularization terms separately.

4.1. Performance measures

4.1.1. Endpoint error

The endpoint error [21] is used to evaluate the motion estimation accuracy. For each pixel n, the endpoint error is defined as $e_n = \sqrt{[\boldsymbol{u}(n) - \hat{\boldsymbol{u}}(n)]^2 + [\boldsymbol{v}(n) - \hat{\boldsymbol{v}}(n)]^2}$, where $\boldsymbol{u}(n), \boldsymbol{v}(n)$ and $\hat{\boldsymbol{u}}(n), \hat{\boldsymbol{v}}(n)$ are the true and estimated horizontal and vertical displacements at pixel n.

4.1.2. Strain

Following the method studied in [22], we measure along the longitudinal direction the deformation of the myocardium with respect to its original shape. If d_0 denotes the distance between adjacent points located in the first frame and d_k the same distance in the kth frame, strain values can be defined as $s_k = d_k/d_0 - 1$, for $k = 1, ..., M$ with M the length of the image sequence [22].

4.2. Realistic Simulations

4.2.1. Simulation scenario

In this work, we consider two sequences of realistic simulated B-mode US data with available ground-truth generated using the scenario described in [22]. Both sequences contain 34 images (of size 224×208, with a pixel size of 0.7×0.6 mm^2, and a frame rate $\in [21, 23]$ Hz) that span a full cardiac cycle and represent dilated cardiomiopathy cases with synchronous (*i.e.*, sync) and dyssynchronous (*i.e.*, LBBB) activation patterns [22][4]. The LBBB sequence was used for training the dictionary whereas the tests were conducted on the sync sequence.

4.2.2. Simulation results

The parameters used in the DL step were selected by cross-validation and fixed for all simulations. More precisely, the patch size was set to $w = 16 \times 16$ pixels, the number of atoms in the dictionary was $n_a = 384$ and the maximum number of non-zero coefficients was adjusted to $K = 5$. The horizontal and vertical motion dictionaries were learned separately from patches of the LBBB sequence (see Section 4.2).

The sparse coding and motion estimation steps require the adjustment of the two regularization parameters λ_s and λ_d. The spatial regularization parameter was fixed to $\lambda_s = 0.1$ after being varied in the interval $[0.01, 10]$. For each outer iteration of the proposed method, λ_d was logarithmically increased from 10^{-3} to 10^2 (see Section 3) in 6 iterations.

Cross-validation was also used to adjust the parameters of the BM and B-spline methods. For the B-spline algorithm, the mesh window size between the B-spline control points was set to $w_{\text{B-spline}} = 15 \times 15$ and the spatial regularization parameter was set to $\lambda_{\text{B-spline}} = 3$ to avoid too much deformation. The window size for the BM algorithm was $w_{\text{BM}} = 32 \times 32$.

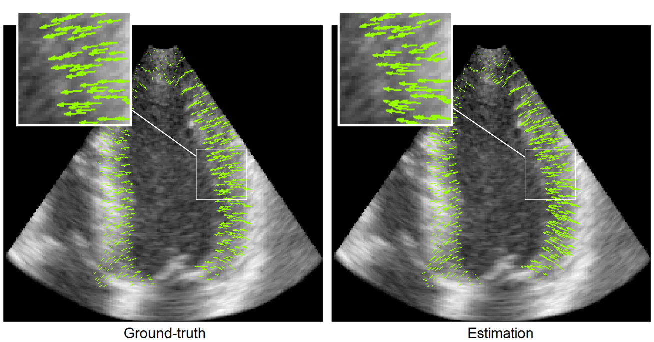

Fig. 1: Ground-truth and estimated meshes of the 10th frame of the sync sequence.

Fig. 1 compares a typical example of an estimated systolic motion field (sync sequence) obtained using the proposed method to the corresponding true displacement meshes. It shows that the estimated motion field is qualitatively consistent with the ground-truth. This performance is complemented by more quantitative results summarized in Table 1. The proposed method clearly performs better than the two other algorithms providing smaller average endpoint errors and smaller estimated standard deviations (calculated for the entire sequence). Table 1 also shows that the proposed combination of both regularizations outperforms the use of sparse ($\lambda_s = 0$) or spatial ($\lambda_d = 0$) regularizations alone.

Method	Proposed	B-spline	BM	Sparse	Spatial
Error	**0.199±0.089**	0.713±0.276	0.985±0.441	0.27±0.19	0.33±0.19

Table 1: Average endpoint error for the simulation sequence sync.

In order to have a more detailed performance analysis during the cardiac cycle, Fig. 2 shows the time evolution of the estimates and the estimated mean strain values. The proposed method outperforms the B-spline and BM algorithms for all frames. Moreover, the differences in estimation accuracy between the beginning (large displacements) and the end (small displacements) of the cardiac cycle are less pronounced, which is an interesting property of the proposed method. Note that a coarse-to-fine estimation scheme was employed for the B-spline method in order to cope with large displacements. However, this multi-resolution scheme was not used for the BM and proposed methods.

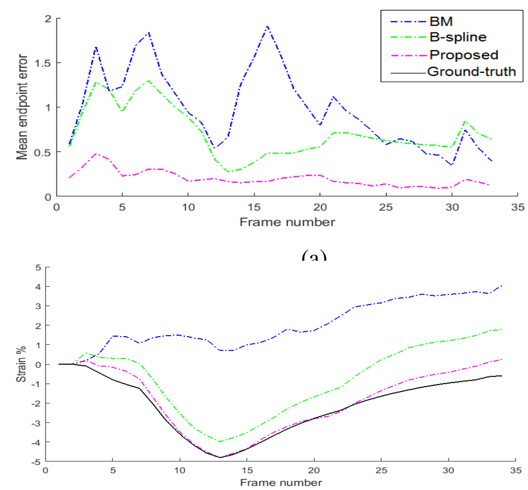

(b)

Fig. 2: Mean endpoint error (a) and mean longitudinal strain values (b) for the sync sequence.

5. CONCLUSIONS

This paper studied a new method for cardiac motion estimation in 2D US images. This method used a similarity measure based on the multiplicative Rayleigh noise assumption penalized by spatial and sparse regularizations. The sparse regularization was based on a dictionary of typical motion vectors computed from realistic images with controlled ground truth. The performance in terms of motion and strain accuracies was very competitive with respect to state-of-the-art methods. For future work, it would be interesting to perform more extensive simulations, *e.g.*, based on *in vivo* data. Another possible prospect is to consider potential deviations in the data fidelity and regularization terms for robust motion estimation.

[4]The data and related papers can be found at https://team.inria.fr/asclepios/data/straus/.

6. REFERENCES

[1] T. P. Abraham, V. L. Dimaano, and H. Liang, "Role of tissue Doppler and strain echocardiography in current clinical practice," *Circulation*, vol. 116, no. 22, pp. 2597–2609, 2007.

[2] P. Baraldi, A. Sarti, C. Lamberti, A. Prandini, and F. Sgallari, "Evaluation of differential optical flow techniques on synthesized echo images," *IEEE Trans. Biomed. Eng.*, vol. 43, no. 3, pp. 259–272, 1996.

[3] A. Myronenko, X. Song, and D. Sahn, *Maximum Likelihood Motion Estimation in 3D Echocardiography through Non-rigid Registration in Spherical Coordinates*, vol. 5528 of *Lecture Notes in Computer Science*, chapter 46, pp. 427–436, Springer Berlin Heidelberg, 2009.

[4] A. Elen, C. Hon Fai, D. Loeckx, G. Hang, P. Claus, P. Suetens, F. Maes, and J. D'Hooge, "Three-dimensional cardiac strain estimation using spatio-temporal elastic registration of ultrasound images: A feasibility study," *IEEE Trans. Med. Imaging*, vol. 27, no. 11, pp. 1580–1591, 2008.

[5] M.J. Ledesma-Carbayo, J. Kybic, M. Desco, A. Santos, M. Suhling, P. Hunziker, and M. Unser, "Spatio-temporal nonrigid registration for ultrasound cardiac motion estimation," *IEEE Trans. Med. Imaging*, vol. 24, no. 9, pp. 1113–1126, 2005.

[6] M. Elad and M. Aharon, "Image denoising via sparse and redundant representations over learned dictionaries," *IEEE Trans. Image Process.*, vol. 15, no. 12, pp. 3736–3745, Dec 2006.

[7] W. Dong, X. Li, L. Zhang, and G. Shi, "Sparsity-based image denoising via dictionary learning and structural clustering," in *Proc. IEEE Conf. Comput. Vision and Pattern Recognition*, Providence, RI, June 2011, pp. 457–464.

[8] Y. Pati, R. Rezaiifar, and P. Krishnaprasad, "Orthogonal matching pursuit: recursive function approximation with application to wavelet decomposition," in *Proc. 27th Asilomar Conf. Signals, Syst. and Comput.*, Pacific Grove, CA, 1993, pp. 2391–2398.

[9] R. Tibshirani, "Regression shrinkage and selection via the lasso," *Journal of the Royal Statistical Society*, vol. 58, no. 1, pp. 267–88, 1996.

[10] J. Mairal, F. Bach, J. Ponce, and G. Sapiro, "Online dictionary learning for sparse coding," in *Proc. 26th Annu. Int. Conf. Mach. Learning (ICML '09)*, New York, NY, USA, 2009, pp. 689–696, ACM.

[11] M. Aharon, Elad, M., and A. Bruckstein, "K-SVD: An algorithm for designing overcomplete dictionaries for sparse representation," *IEEE Trans. Signal Process.*, vol. 54, no. 11, pp. 4311–4322, 2006.

[12] X. Shen and Y. Wu, "Sparsity model for robust optical flow estimation at motion discontinuities," in *Proc. IEEE Conf. Comput. Vision and Pattern Recognition*, San Francisco, CA, 2010, pp. 2456–2463.

[13] K. Jia and X. Wang, "Optical flow estimation using learned sparse model," in *Proc. IEEE Int. Conf. Comput. Vision*, Barcelona, Spain, 2011, pp. 2391–2398.

[14] B. Cohen and I. Dinstein, "New maximum likelihood motion estimation schemes for noisy ultrasound images," *Pattern Recognition*, vol. 35, no. 2, pp. 455–463, 2002.

[15] K. Kaluzynski, X. Chen, S. Y. Emelianov, A. R. Skovoroda, and M. O'Donnell, "Strain rate imaging using two-dimensional speckle tracking," *IEEE Trans. Ultrason. Ferroelectr. Freq. Control*, vol. 48, no. 4, pp. 1111–1123, July 2001.

[16] N. Ouzir, A. Basarab, H. Liebgott, B. Harbaoui, and J.-Y. Tourneret, "Motion estimation in echocardiography using sparse representation and dictionary learning," *submitted to IEEE Trans. Image Process.*, 2017.

[17] F. Viola and W. F. Walker, "A comparison of the performance of time-delay estimators in medical ultrasound," *IEEE Trans. Ultrason. Ferroelectr. Freq. Control*, vol. 50, no. 4, pp. 392–401, April 2003.

[18] J.W. Goodman, *Speckle Phenomena in Optics: Theory and Applications*, Roberts & Company, 2007.

[19] B. K. P. Horn and B. G. Schunck, "Determining optical flow," *Artificial Intelligence*, vol. 17, no. 1, pp. 185–203, 1981.

[20] J. Sulam and M. Elad, *Expected patch log likelihood with a sparse prior*, pp. 99–111, Springer Berlin Heidelberg, 2015.

[21] M. Alessandrini, A. Basarab, H. Liebgott, and O. Bernard, "Myocardial motion estimation from medical images using the monogenic signal," *IEEE Trans. Image Process.*, vol. 22, no. 3, pp. 1084–1095, 2013.

[22] M. Alessandrini, B. Heyde, S. Queiros, S. Cygan, M. Zontak, O. Somphone, O. Bernard, M. De Craene, M. O'Donnell, and J. D'hooge, "Detailed evaluation of five 3D speckle tracking algorithms using synthetic echocardiographic recordings," *IEEE Trans. Med. Imaging*, vol. 35, no. 8, pp. 1915–1926, Aug. 2016.